Shear Capacity of Stud-Groove Connector in Glulam-concrete Composite Structure

Lan Xie,[a] Guojing He,[a,*] Xiaodong (Alice) Wang,[b] Per Johan Gustafsson,[c] Roberto Crocetti,[c] Liping Chen,[d] Li Li,[a] and Wenhui Xie [a]

A timber-concrete composite structure (TCC) is economically and environmentally friendly. One of the key design points of this kind of structure is to ensure the reliability of the shear connectors. The objective of this paper is to study the mechanical property of stud-groove-type connectors and to provide shear capacity equations for stud-groove connectors in timber-concrete composite structures. Based on the Johansen Yield Theory (European Yield Model), some mechanical models and capacity equations for stud-groove-type connectors in timber-concrete structures were studied. Push-out specimens with different parameters (stud diameter, stud length, groove width, and groove depth) were tested to obtain the shear capacity and slip modulus. The experimental strengths were used to validate equations given in the paper. The shear capacity and slip modulus of stud-groove-type connectors was in direct proportion to the diameter of studs and the dimension of the groove. Comparison between the theoretical and the experimental shear strength results showed reasonable agreement. The highlight of this study on shear capacity equations could significantly reduce the push-out tests before investigating the other properties of TCC.

*Contact information: a: Department of Civil Engineering and Mechanics, Central South University of Forestry and Technology, 498 Shaoshan Road, Changsha, Hunan 410004 China; b: Wood Technology and Engineering, Luleå University of Technology, Forskargatan 1, SE-931 87 Skellefteå, Sweden; c: Division of Structural Mechanics, Lund University, Box 188, 221 00 Lund, Sweden, d: Hunan Huagang Planning and Design Research Institute Co., Ltd., 45 Chiling Road, Changsha, Hunan 410004 China; * Corresponding author: lily.csuft.xie@gmail.com; cegjhe@hotmail.com*

INTRODUCTION

Timber-concrete composite (TCC) structures (*e.g.* floors, buildings, and bridges) have become increasingly popular due to their lower carbon dioxide emissions, low cost, and energy conservation (Natterer 1997; Wegener 1997). Several researchers have performed experimental studies on TCC structures (Grantham *et al.* 2004; Clouston *et al.* 2005). There are various kinds of connectors that have been developed in many areas of the world in the last 80 years, such as stud or screw connectors, dowels, and grooves that are cut in the timber and filled with concrete. Researchers have found that making the shear connectors sufficiently stiff (and strong) is a key point to achieve a structurally sound TCC structure (Yeoh *et al.* 2011a). Yeoh *et al*. (2008, 2009) tested variations of typical notched connections that were also inserted with coach screws and toothed metal plate fasteners. The results obtained from their experiments indicated that both a 300-mm rectangular notch and toothed metal plate connections had the best strength qualities.

Analytical design formulas for the shear strength evaluation of notched connections were derived for the failure of concrete and LVL (Yeoh *et al.* 2011b). Slip-block tests were performed with notch connectors of various parameters (without coach screws) to get the characterization of shear connection between timber and concrete (Hehl *et al.* 2014). Four-point bending tests were performed on the rectangular notches and sinusoidal notched wave connectors to study the structural behavior of beech-LVL-concrete composite structure (Boccadoro and Frangi 2014). The mechanical properties of different connectors were investigated and some full-scale timber-concrete composite slabs were also tested (Crocetti *et al*. 2015).

Most previous studies have been focused on the experimental testing of the connectors of TCC. It is tedious and wasteful for every researcher to do recurrent push-out tests before investigating the other properties of TCC. Therefore, it is very desirable to develop mechanics-based formulas to evaluate the shear strength of TCC connectors. Moreover, there has been little research done on TCC with Chinese timber materials. Also, the corresponding information in literature and code does not provide enough information on how to modify the design of timber-concrete composite structures.

In the present study, both the failure mode and the shear capacity of stud-groove type connectors were studied according to the Johansen Yield Theory (Johansen 1962). Some experiments on TCC were done to provide load-slip curves to analyze connector properties of timber-concrete composite structures with slips. The TCC push-out components with different parameters of stud-groove were tested to predict the mechanical properties of the connector. The specific objective of this paper was to investigate the mechanical properties of stud-groove connectors in TCC push-out specimens theoretically and experimentally.

Shear capacity equation

Previous push-out tests have shown that the main failure of TCC push-out specimens with screw or bolt connectors are commonly caused by bending failure or failure due to rigid body rotation of the connectors (Lan 2010; He *et al*. 2016a,b). To do a mechanics-based calculation, it was assumed that the shear failure developed in the concrete at a certain location with no shear failure in the wood and no compressive failure in wood or concrete, apart from local failure at the dowels. Moreover, it was assumed that the shear failure area in the concrete did not carry any load so that the dowels carried the entire load. In Fig. 1, the notation R was used to define the load of dowel. This assumption and this notation is used only during the derivation of the load capacity of the dowel. According to Johansen Yield Theory, assuming the embedment stress behavior of studs in timber and concrete as rigid-plastic, six failure modes either with two plastic hinges, one plastic hinge, or rigid body rotation (Fig. 1) can be obtained. Force equilibrium in the vertical direction gives Eqs. 1(a) through 1(d),

$$f_{h,t}db_1 = f_{h,c}d(a_2 - b_2) = \beta f_{h,t}d(a_2 - b_2)$$

1(a)

$$f_{h,c}db_2 = f_{h,c}da_2$$

1(b)

$$f_{h,t}d(a_1 - b_1) = f_{h,c}d(b_2 - a_2) = \beta f_{h,t}d(b_2 - a_2)$$

1(c)

$$f_{h,t}dp = f_{h,c}d(t_2 - t_1 - a_2) = \beta f_{h,t}d(t_2 - t_1 - a_2)$$

1(d)

where $f_{h,t}$ is the embedment strength in timber (MPa), $f_{h,c}$ represents the embedment strength in concrete (MPa), d is the diameter of stud (mm), a_1, a_2, b_1, b_2, t_1, and t_2 are presented in Fig. 1, p is the penetration depth of the stud in the glulam (mm), and β represents the ratio of embedment strength in concrete and timber (Eq. 2),

$$\beta = \frac{f_{h,c}}{f_{h,t}}$$

(2)
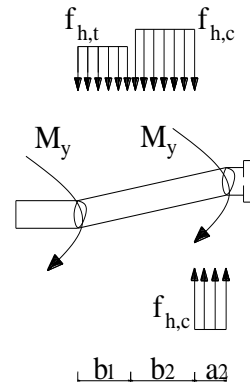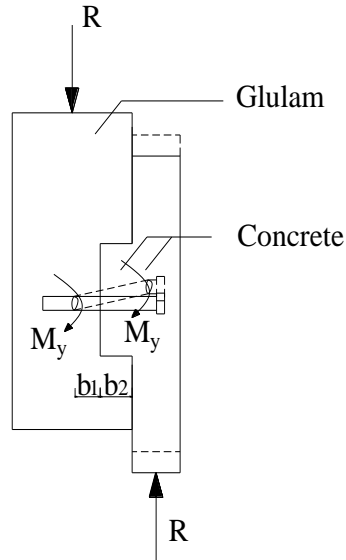
a)
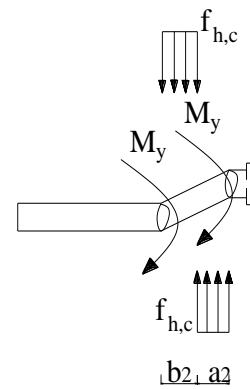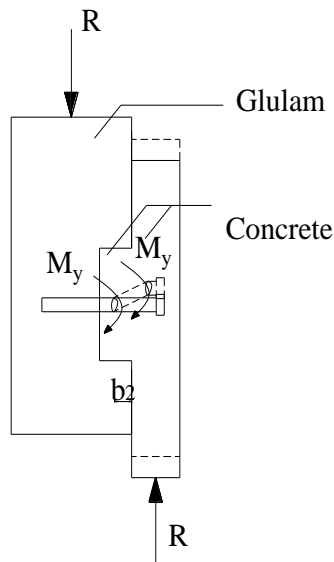
b)
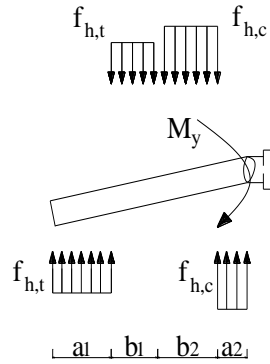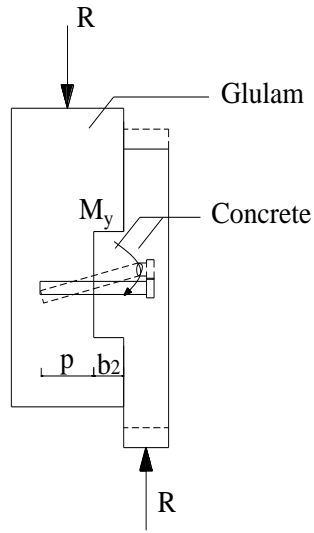
c)
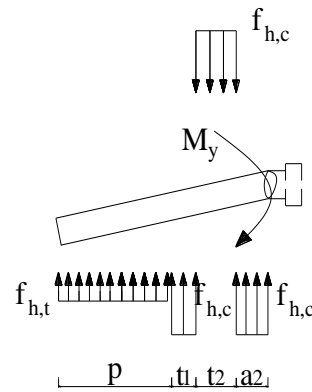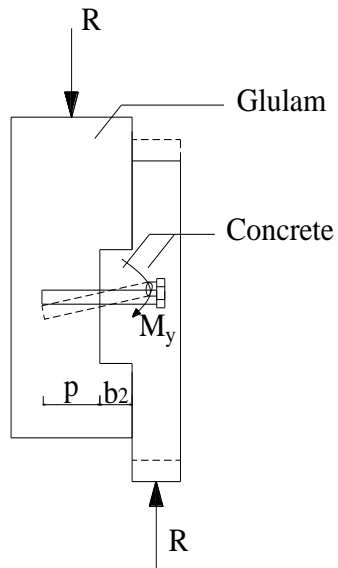
d)
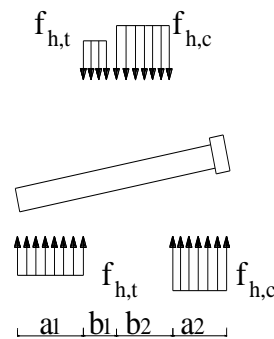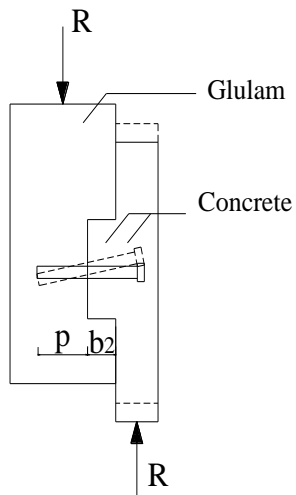
e)
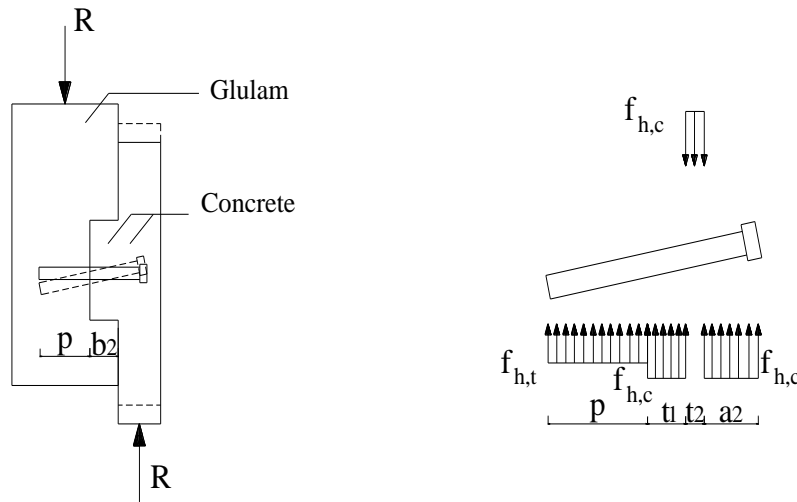
f)

Fig. 1. Mechanism of stud-groove-type connectors failure: a) failure mode with two plastic hinges, one hinge in concrete and another in glulam; b) failure mode with two plastic hinges, both hinges in concrete; c) failure mode with one plastic hinge, with the intersection of stud before and after failure in glulam; d) failure mode with one plastic hinge, with the intersection of stud before and after failure in concrete in the groove; e) failure mode with rotation, with the intersection of stud before and after failure in glulam; and f) failure mode with rotation, with the intersection of stud before and after failure in concrete in the groove

At the plastic hinge in Fig. 1, the maximum bending moment is M_y (N • mm), According to the moment balance, which corresponded to the failure modes, the equilibrium expressions were obtained as Eqs. 3(a) through 3(d),

$$2M_y = -f_{h,t}d\frac{b_1^2}{2} - f_{h,c}db_2(b_1+\frac{b_2}{2}) + f_{h,c}da_2(b_1+b_2+\frac{a_2}{2})$$

3(a)

$$2M_y = -f_{h,c}d\frac{b_2^2}{2} + f_{h,c}da_2(b_2+\frac{a_2}{2})$$

3(b)

$$M_y = -f_{h,t}da_1(\frac{a_1}{2}+b_1+b_2+a_2) + f_{h,t}db_1(\frac{b_1}{2}+b_2+a_2) + f_{h,c}db_2(\frac{b_2}{2}+a_2) - f_{h,c}d\frac{a_2^2}{2}$$

3(c)

$$M_y = -f_{h,c}d\frac{a_2^2}{2} + f_{h,c}dt_2(a_2+\frac{t_2}{2}) - f_{h,c}dt_1(a_2+t_2+\frac{t_1}{2}) - f_{h,t}dp(a_2+t_1+t_2+\frac{p}{2})$$

3(d)

where the variables are the same as aforementioned.

From Eq. 1(a), it is easy to see the relation that $b_1 = \beta(a_2-b_2)$. From Eq. 1(b), it is easy to see the relation that $b_2 = a_2$. From Eq. 1(c) and Fig. 1(c), it is easy to see the relations of $a_1 = \dfrac{p+\beta(b_2-a_2)}{2}$, $b_1 = p-a_1 = \dfrac{p-\beta(b_2-a_2)}{2}$. From formula 1(d) and Fig. 1(d), it is easy to see the relations of $t_1 = \dfrac{b_2-a_2-p/\beta}{2}$, $t_2 = b_2-t_1 = \dfrac{a_2+b_2+p/\beta}{2}$. From

Figs. 1(e) and 1(f), the relations of $a_2 = l - p - b_2$ can be seen. The following equations were subsequently obtained,

$$a_2 = \frac{b_2(\beta-1)}{1+\beta} + \sqrt{\frac{4M_y}{\beta f_{h,t}d(1+\beta)} + \frac{2b_2^2}{1+\beta}}$$

4(a)

$$a_2 = \sqrt{\frac{2M_y}{\beta f_{h,t}d}}$$

4(b)

$$a_2 = -\frac{4b_2+p}{4} + \sqrt{\frac{2M_y}{\beta f_{h,t}d} + \frac{8+\beta}{16\beta} + b_2(2b_2+p)}$$

4(c)

$$a_2 = -\frac{\beta b_2+p}{3\beta} + \sqrt{(\frac{p+\beta b_2}{3\beta})^2 + \frac{2b_2p+2p^2+b_2^2\beta}{3\beta} + \frac{4\beta M_y - p^2 d f_{h,t}}{3\beta^2 f_{h,t}d}}$$

4(d)

where *l* is the length of the stud (mm) shown in Fig. 1, and the other variables are the same as aforementioned. The shear resistance of the stud for the failure modes presented in Fig. 1 can be written as Eq. 5,

$$R = \beta f_{h,t}d a_2$$

(5)

which was finally obtained as Eqs. 6(a) through 6(e),

$$R = \beta f_{h,t}d[\frac{b_2(\beta-1)}{1+\beta} + \sqrt{\frac{4M_y}{\beta f_{h,t}d(1+\beta)} + \frac{2b_2^2}{1+\beta}}]$$

6(a)

$$R = \beta f_{h,t}d\sqrt{\frac{2M_y}{\beta f_{h,t}d}}$$

6(b)

$$R = \beta f_{h,t}d[-\frac{4b_2+p}{4} + \sqrt{\frac{2M_y}{\beta f_{h,t}d} + \frac{8+\beta}{16\beta} + b_2(2b_2+p)}]$$

6(c)

$$R = \beta f_{h,t}d\left[-\frac{\beta b_2+p}{3\beta} + \sqrt{(\frac{p+\beta b_2}{3\beta})^2 + \frac{2b_2p+2p^2+b_2^2\beta}{3\beta} + \frac{4\beta M_y - p^2 d f_{h,t}}{3\beta^2 f_{h,t}d}}\right]$$

6(d)

$$R = \beta f_{h,t}d(l-p-b_2)$$

6(e)

The variables are the same as aforementioned.

In the mechanical models previously stated, the friction force is not taken into account because it is very small (Li *et al.* 2014). Therefore, Eq. 6 is a conservative estimate value for the shear capacity of stud-groove-type connectors in the TCC structure. Also, the equation did not consider the capacity provided by concrete. The load capacity of the dowel and the concrete should be added. They are added because the load resistance *R* of the dowel is (at the least theoretically and in accordance with the Johansen theory, which is assuming ideal plastic performance) the same for all magnitudes of the

deformation, also for the magnitude of deformation at which shear fracture develops in the concrete. The total shear capacity can be presented as Eq. 7,

$$F = R + 0.51\sqrt{f_{cu}}bh$$

(7)

where, b and h are the width and height of concrete in the groove (mm), respectively, R is presented in Eq. 6.

According to the European standard (EN 1995-1 (2004) for bolts and laminated veneer lumber (LVL), the embedment strength can be conservatively estimated from Eq. 8,

$$f_{h,t} = 0.082(1 - 0.01d)\rho$$

(8)

where, p is the characteristic timber density (kg/m^3). The characteristic value for the yield moment can be estimated from Eq. 9,

$$M_y = 0.3f_u d^{2.6}$$

(9)

where, f_u is the characteristic tensile strength of the stud (N/mm^2).

Because the studs fail in the concrete when the composite structure reaches its ultimate capacity, information about the embedment strength of the concrete is needed. The embedment strength is defined as,

$$f_{h,c} = \frac{P_u}{dh_c}$$

(10)

where, d is the diameter of the stud (mm), h_c is the total length in the concrete block including the head length of the stud (mm), and P_u is the shear force resistance of a bolt in a concrete encasement (N), which was assumed according to Eurocode 4 EN 1994-1-1 (2004).

$$P_u = 0.29d^2\sqrt{f_{ck}E_{cm}}$$

(11)

In Eq. 11, d is the diameter of the stud, f_{ck} is the characteristic cylinder compressive strength of the concrete (N/mm^2), and E_{cm} is the mean secant modulus of elasticity of concrete.

EXPERIMENTAL

Materials
Glulam

The glulam used in the experiments was made of Xing'an larch (*Larix*), which is appropriate for applications in engineering. Some Xing'an larch boards were glued with aqueous polyurethane adhesive. The adhesive was purchased from Nanjing Skybamboo Science & Technology Industry Co., Ltd, Nanjing, China.

According to the standardized test method used for timber structures, GB/T 50329 (2002), six specimens with dimensions of 60 mm × 60 mm × 300 mm were tested to obtain the mechanical properties of timber (Fig. 2). The compresive strength mean value that was obtained from the tests was 49.3 Mpa, with the coefficient of variation as 0.011,

and the moisture of wood was 11.8%. (Chen 2015). Next, six specimens with the dimensions of 20 mm × 20 mm × 20 mm were tested to obtain the density of the timber. The mean density of timber was 562.5 kg/m^3.
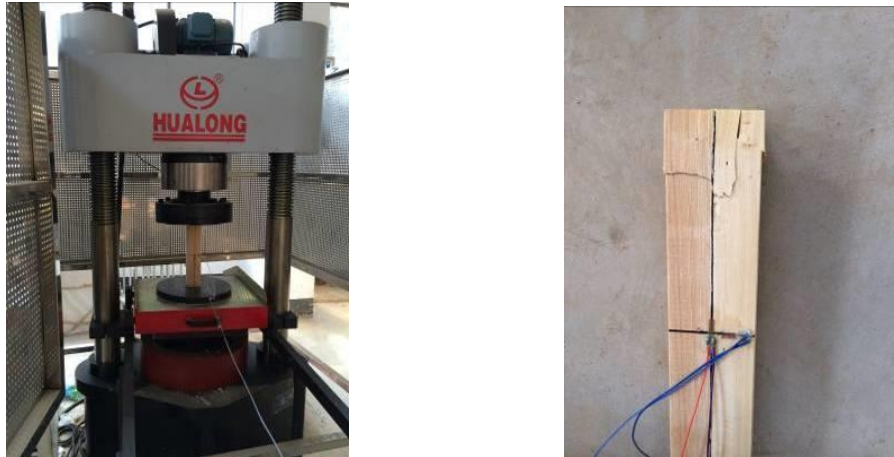
Fig. 2. Compressive strength tests of timber

Concrete

According to the standardized test method used for concrete structures, GB 50010-2010 (2010), 3 specimens with dimensions of 150 mm × 150 mm × 150 mm were tested to obtain the mechanical properties of concrete (Fig. 3). All concrete blocks were made in a laboratory at Central South University of Forestry and Technology. The cement "32.5," sand, and pebble were bought from a local building materials factory (Steel Mill) in Changsha, China. The expected strength class of the concrete was C30. The actual mean strength of the concrete specimens was determined by the testing shown in Fig. 3 as 31.10 MPa.

Fig. 3. Compressive strength tests of concrete

Steel

The smooth steel studs used in the composite specimens were bought from Hebei Jinan Standard Component Industry Co., Ltd., Jinan, China. The ultimate tensile strength of the steel stud was 400 MPa and the yield strength was 320 Mpa, which was provided by the industry. The steel studs were hammered into the timber before the concrete was poured.

Design of Push-out Specimens

The push-out specimens consisted of two sides of concrete and one timber block. Grooves were cut in the timber with different dimensions (Fig. 4). After cutting holes in the timber, studs with various parameters (Table 1) were driven into the timber and then concrete was poured. The dimensions of the concrete component in the push-out specimen were 60 mm × 300 mm × 400 mm, and those of the timber were 160 mm × 300 mm × 400 mm. No slip membrane was placed in the specimens. Three specimens in each series were tested. The dimensions of each of these samples are shown in Table 1.

Vertical View

Side View

Notice:
(1) x=300-2p-2d;
(2) concrete is poured in the groove

Plan View
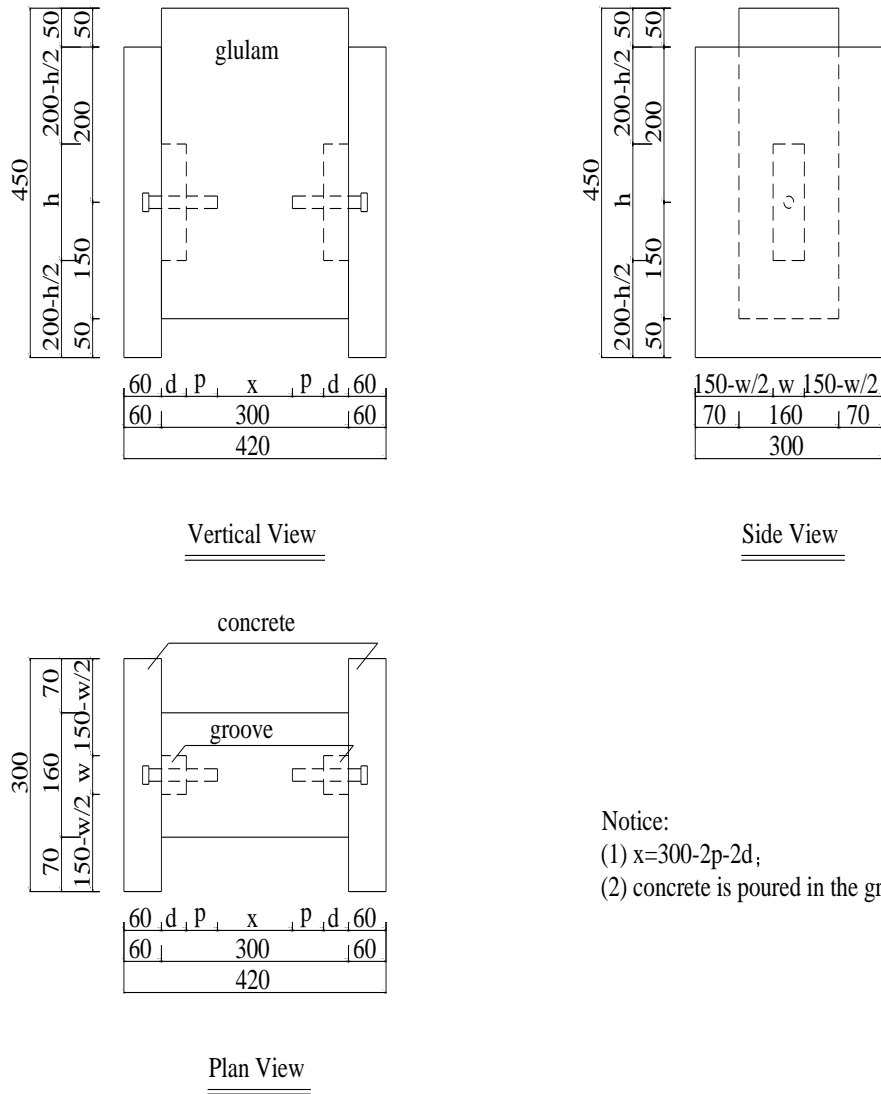
Fig. 4. Drawing of timber-concrete composite push-out samples (Unit:mm)

Table 1. Dimensions of Samples

No.	Groove			Stud		Penetration depth (p) (mm)
	Height (h) (mm)	Width (w) (mm)	Depth (d) (mm)	Diameter (mm)	Length (mm)	
T-1	150	60	50	16	130	40
T-2	150	60	20	16	130	70
T-3	150	40	50	16	130	40
T-4	150	80	50	16	130	40
T-5	150	60	50	13	130	40
T-6	150	60	50	10	110	60
* The stud length is the total length, including the head length						

Methods

The standard BS EN 26891 (1991) was referred to for the statically loaded tests of the TCC specimens but without the unloading part. The loading rate were controlled according to EN 26891. Tests were applied by displacement control until 15 mm or structure fail.

A universal testing machine (WEW-2000, Shenzhen SANS Materials Testing Co., Ltd., Shenzhen, China) was used to apply the load to the top surface of a loading steel plate which was on the timber in TCC samples. The applied loads were then recorded. Four displacement gauges were used to measure the interlamination slip between the concrete and timber (Fig. 5).

(a) Displacement gauge arrangement   (b) Apparatus used on the tests
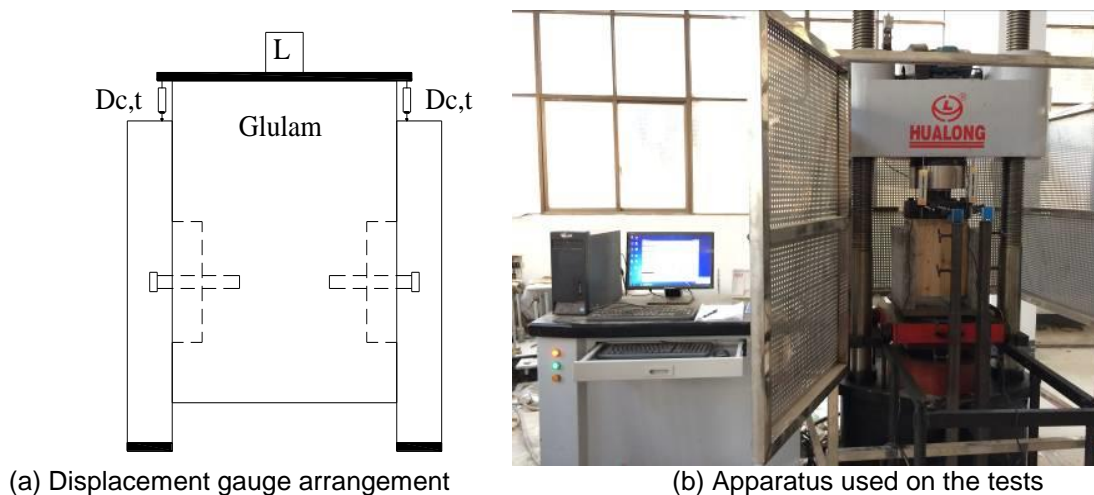
Fig. 5. Apparatus used on the tests

RESULTS AND DISCUSSION

Experimental Results

The load-slip curves for all series of specimens are presented with the corresponding ultimate load (F_{max}), slip (δ), and slip modulus (K_S). These parameters are usually necessary for the design of the timber-concrete composite structures (Dias 2005). The mean values and coefficient of variations of the important data were obtained from the tests, and they are presented in Table 2 and Fig. 6. The initial slip and slip modulus

can be calculated according to BS EN 26891 (1991), as normal distribution was assumed. To validate the experimental strength to aforementioned equation, the characteristic values were calculated according to SS EN 14358 (2016).

The mechanical behavior of the groove and stud-type fasteners showed an obvious non-linear property for all series. At the beginning of the tests, there was a slight slip between the timber and concrete. As the load increased, some cracks appeared in the timber block, and the lamination slip between timber and concrete occurred until the specimens failed. Finally, the timber and concrete released from each other and the studs bent or rotated and then failed (Fig. 7).

Table 2. Results for Joints with Stud-Groove-Type Fasteners

No.	Strength F_{max} (kN)			Initial Slip δ_i (mm)			Slip Modulus K_s (10^3kN/mm)		
	Value	Mean/ Characteristic Value	Cov*	Value	Mean Value	Cov*	Value	Mean Value	Cov*
T-1-1	92.10			0.48			54.74		
T-1-2	92.86	92.19/90.22	0.01	0.49	0.45	0.12	63.09	62.32	0.12
T-1-3	91.62			0.39			69.13		
T-2-1	85.62			0.65			43.53		
T-2-2	82.86	83.53/77.69	0.02	0.66	0.64	0.04	42.83	43.57	0.02
T-2-3	82.10			0.61			44.36		
T-3-1	68.00			0.43			41.73		
T-3-2	66.76	68/64.09	0.02	0.38	0.48	0.27	47.43	41.71	0.14
T-3-3	69.24			0.63			35.97		
T-4-1	98.70			0.43			68.71		
T-4-2	100.34	98.73/93.69	0.02	0.32	0.42	0.24	86.97	71.13	0.21
T-4-3	97.14			0.52			57.72		
T-5-1	68.84			0.52			38.78		
T-5-2	71.28	68.84/61.15	0.04	0.62	0.52	0.20	36.78	40.80	0.13
T-5-3	66.40			0.41			46.85		
T-6-1	60.74			0.65			31.30		
T-6-2	61.96	60.74/56.9	0.02	0.72	0.63	0.16	31.13	33.32	0.11
T-6-3	59.52			0.52			37.53		
*Coefficient of variation									
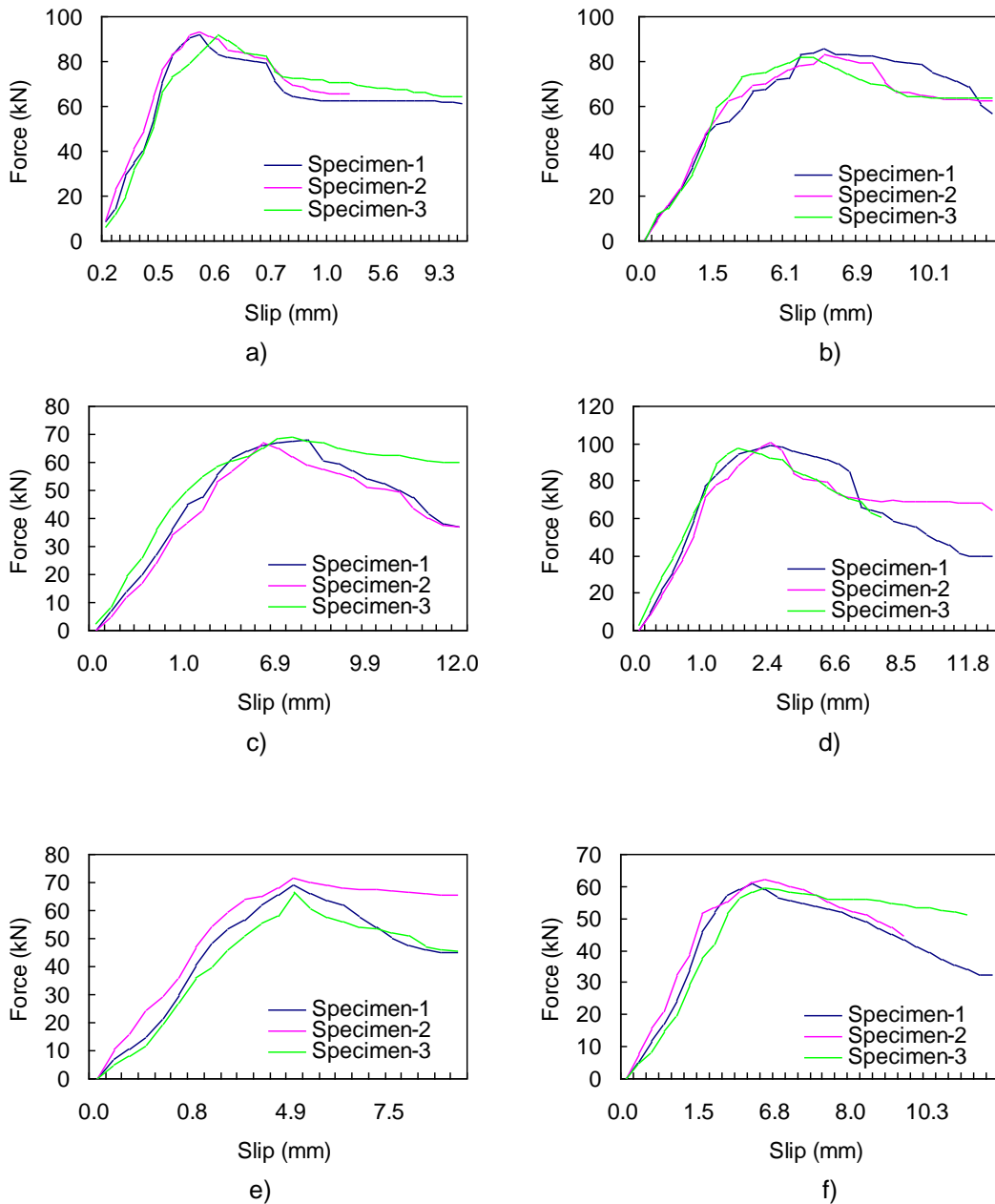
Fig. 6. Load-slip curves for all test groups: a) T-1; b) T-2; c) T-3; d) T-4; e) T-5; and f) T-6
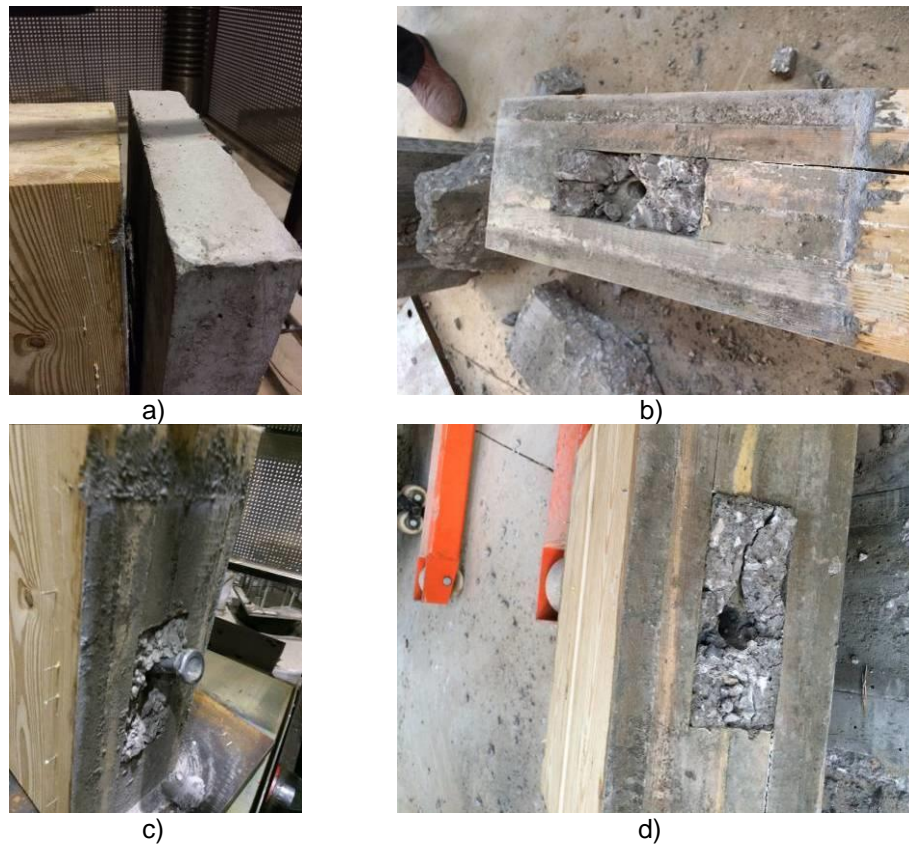
Fig. 7. Failure modes for timber-concrete composite specimens with stud-groove: a) timber is away from the concrete; b) cracks on timber; c) stud deformed and failed; and d) concrete failed

Influence of stud diameter

Table 3 shows the mean values for the results of T-2 to T-6 specimens relative to that of T-1 specimens. The strength and slip modulus values were almost proportional to the square of stud diameter.

The mechanical property law of the capacity and slip modulus of studs and groove-type connectors obtained from the experiments was in accordance with that of Eq. 6, which showed that the shear capacity of the connector was in direct proportion to the diameter of the stud.

Table 3. Relative Influence of Dimension on Results for Groove and Studs

No.	Groove			Stud		Strength (kN)	Initial Slip (mm)	Slip Modulus (kN/mm)
	h (mm)	W (mm)	d (mm)	Diameter (mm)	Length (mm)			
T-1	150	60	50	16	130	1.00	1.00	1.00
T-2	150	60	20	16	130	0.91	1.42	0.70
T-3	150	40	50	16	130	0.74	1.07	0.67
T-4	150	80	50	16	130	1.07	0.93	1.14
T-5	150	60	50	13	130	0.75	1.16	0.65
T-6	150	60	50	10	110	0.66	1.40	0.53

Influence of groove dimension

The shear capacity and slip modulus of the stud-groove type connector were almost proportional to the width of the groove and proportional to the depth of the groove. This conclusion did not agree with Eq. 6, which showed that the capacity of the connector decreased as the dimension of the groove increased. Theoretically, a smaller groove will decrease the stiffness of the structure and the capacity. The reason for the improvement of the connector capacity was that the concrete that was poured in the timber groove provided strength. The dimension of the groove equaled the concrete size. Therefore, it can be said that the dimension of the groove is in direct proportion to the capacity of studs-groove-type connectors, which agrees with Eq. 7.

Validation of Shear Capacity Equation

With p = 562.5 kg/m^3 and f_u = 400 MPa, the main experimental and theoretical results are presented in Table 4.

Table 4. Comparison of Test and Theory Results

No.	F_t (kN)	F_{mean} (kN)	Δ_1 (%)	Δ_2 (%)
T-1	95.32	92.19	-1.92	11.21
T-2	85.58	83.53	7.74	15.54
T-3	64.04	68.00	5.66	16.40
T-4	98.17	98.73	-1.03	6.48
T-5	70.65	68.84	-2.13	0.66
T-6	64.70	60.74	6.28	6.70

*F_t = theoretical shear capacity based on Eq. 7; F_{mean} = mean test result obtained from the experiment; Δ_1 = (F_{mean} - F_t) / F_{mean} x 100; Δ_2 = (F_{mean} - F_{t2}) / F_{mean} x 100; and F_{t2} = theoretical shear capacity based on Eq. 7 with f_{hc}=4/5f_c (Colajanni *et al.* 2015, 2017)

The comparison of experimental and theoretical results based on the European Yield Model indicated that the capacity equation based on the failure model could predict the shear capacity of stud-groove connections, with an error less than 8%. The error calculated with f_{hc}=4/5f_c according to the references (Colajanni *et al.* 2015, 2017) was less than 17%. The capacity equation can provide conservative results for design.

CONCLUSIONS

1. This paper theoretically and experimentally investigated the mechanical properties of stud-groove connectors in TCC push-out specimens and provided the shear capacity equation of stud-groove connectors in TCC structure. It is economically advantageous to use the shear capacity equation to predict the shear strength of connectors rather than conducting a large amount of experiments.

2. Six mechanical failure modes were presented, and some capacity equations of stud-groove type connectors were provided. The capacity equations for stud-groove type connectors were conservative because the friction and capacity provided by the concrete was not considered.

3. Under the load, the TCC specimens failed with the lamination slip between timber and concrete. Studs reached the bending yield and cracks appeared in timber blocks when the specimens failed.

4. In accordance to the theory, the experimental shear capacity and slip modulus of stud-groove-type connectors was in direct proportion to the diameter of studs.

5. The shear capacity and slip modulus of the stud-groove-type connectors were in direct proportion to the dimension of the grooves according to tests, which is in opposition to the theory. This was due to the concrete that was present in the grooves.

6. The shear capacity equations were based on the failure modes presented in the paper, which accurately predicted the conservative results of the connections.

ACKNOWLEDGMENTS

REFERENCES CITED

Boccadoro, L., and Frangi, A. (2014). "Experimental analysis of the structural behavior of timber-concrete composite slabs made of beech-laminated veneer lumber," *Journal of Performance of Constructed Facilities* 28(6). DOI: 10.1061/(ASCE)CF.1943-5509.0000552.

BS EN 26891 (1991). "Timber structures-joints made with mechanical fasteners - General principles for the determination of strength and deformation characteristics," British Standards Institution, London, UK.

Clouston, P., Bathon, L., and Schreyer, A. (2005). "Shear and bending performance of a novel wood-concrete composite system," *Journal of Structural Engineering* 131(9), 1404-1412. DOI: 10.1061/(ASCE)0733-9445(2005)131:9(1404)

Chen, L. (2015). *Study on Mechanical Property of Notch-stud Connectors for Timber-Concrete Composite Beams*, Master's Thesis, Central South University of Forestry and Technology, Changsha, China.

Colajanni, P., La Mendola, L., Latour, M., Monaco, A., and Rizzano, G. (2017). "Analytical prediction of the shear connection capacity in composite steel–concrete trussed beams," *Materials and Structures/Materiaux et Constructions* 50 (1), art. no. 48

Colajanni, P., La Mendola, L., Latour, M., Monaco, A., Rizzano, G. (2015). "FEM analysis of push-out test response of Hybrid Steel Trussed Concrete Beams (HSTCBs)," *Journal of Constructional Steel Research* 111, pp. 88-102.

Crocetti, R., Sartori, T., and Tomasi, R. (2015). "Innovative timber-concrete composite structures with prefabricated FRC slabs," *Journal of Structural Engineering* 141(9). DOI: 10.1061/(ASCE)ST.1943-541X.0001203

Dias, A. M. P. G. (2005). *Mechanical Behavior of Timber-Concrete Joints*, Ph.D Dissertation, Universidad de Coimbra, Coimbra, Portugal.

EN 1994-1-1: Eurocode 4 (2004). "Eurocode 4: Design of composite steel and concrete structures – Part 1-1: General rules and rules for buildings," European Committee for Standardization, Brussels, Belgium.

EN 1995-1: Eurocode 5 (2004). "Design of timber structures-part 1-1: General common rules and rules for buildings," European Committee for Standardization, Brussels, Belgium.

Grantham, R., Enjily, V., Fragiacomo, M., Nogarol, C., Zidaric, I., and Amadio, C. (2004). "Potential upgrade of timber frame buildings in the UK using timber-concrete composites," in: *Proceedings of the 8th World Conference on Timber Engineering* 2, 59-64.

GB/T 50329 (2002). "Standard for methods testing of timber structures," Standardization Administration of China, Beijing, China.

GB 50010-2010 (2010). "Code for design of concrete structures," Standardization Administration of China, Beijing, China.

He, G. J., Xie, L., Wang, A., Yi, J., Peng, L. N., Chen, Z. A., Gustafsson, P. J., and Crocetti, R. (2016a). "Shear behavior study on timber-concrete composite structures with bolts," *BioResources* 11(4), 9205-9218. DOI: 10.15376/biores.11.4.9205-9218

He, G. J., Xie, L., Wang, A., Yi, J., Li, Y. Y., and Xiang, L. L. (2016b). "Study on mechanical property of screw connector for timber-concrete composite structure with interlamination slips," in: *Proceedings of the 11th World Conference on Timber Engineering*, Vienna, Austria.

Hehl, S., Tannert, T., Meena, R., and Vallee, T. (2014). "Experimental and numerical investigations of groove connections for a novel timber-concrete-composite system," *Journal of Performance of Constructed Facilities* 28(6). DOI: 10.1061/(ASCE)CF.1943-5509.0000549

Johansen, K. W. (1962). *Yield-line Theory*, Cement and Concrete Association, London, UK.

Lan, X. (2010). *Experimental Study on Push-out Tests of Screw Connectors for Timber-Concrete Composite Beams*, Master's Thesis, Nanjing University of Technology, Nanjing, China.

Li, Z., Xiao, Y., Wang, R., and Monti, G. (2014). "Studies of nail connectors used in wood frame shear walls with ply-bamboo sheathing panels," *Journal of Materials in Civil Engineering* 27(7). DOI: 10.1061/(ASCE)MT.1943-5533.0001167

Natterer, J. (1997). "Sustainable economy of forestry and value added utilization of forests," in: *Restoration of Forests- Environmental Challenges in Central and Eastern Europe*, R. M. Gutkowski, T. Winnicki (eds.), NATO ASI Ser. 2, Kluwer Academic, Dordrecht, Netherlands, pp. 30, 97-118.

SS EN 14358 (2016). "Timber structures – Calculation and verification of characteristic values," Swedish Standards Institute, Stockholm, Sweden.

Wegener, G. (1997). "Increasing public awareness of contribution of forestry and wood utilization to ecology," in: *Restoration of Forests – Environmental Challenges in Central and Eastern Europe*, R. M. Gutkowski, T. Winnicki (eds.), NATO ASI Ser. 2, Kluwer Academic, Dordrecht, Netherlands, 30, 77-96.

Yeoh, D., Fragiacomo, M., Buchanan, A., Crews, K., Haskell, J., and Deam, B. (2008). "Development of semi-prefabricated timber-concrete composite floors in Australasia," in: *Proceedings of the 10th World Conference on Timber Engineering*, Miyazaki, Japan.

Yeoh, D., Fragiacomo, M., Buchanan, A., and Gerber, C. (2009). "Preliminary research towards a semi-prefabricated LVL-concrete composite floor system for the Australasian market," *Australian Journal of Structural Engineering* 9(3), 1-16.

Yeoh, D., Fragiacomo, M., Franceschi, M., and Boon, K. H. (2011a). "State of the art on timber-concrete composite structures: Literature review," *Journal of Structural Engineering* 137(10), 1085-1095. DOI: 10.1061/(ASCE)ST.1943-541X.0000353

Yeoh, D., Fragiacomo, M., Franceschi, M., and Buchanan, A. (2011b). "Experimental tests of notched and plate connectors for LVL-concrete composite beams," *Journal of Structural Engineering* 137(2), 261-269. DOI: 10.1061/(ASCE)ST.1943-541X.0000288